Available online at www.sciencedirect.com
SCIENCE DIRECT®
International Journal of Mass Spectrometry 240 (2005) 169–182
International Journal of Mass Spectrometry
www.elsevier.com/locate/ijms

The curved-field reflectron: PSD and CID without scanning, stepping or lifting☆

Robert J. Cotter*, Serguei Iltchenko, Dongxia Wang

Middle Atlantic Mass Spectrometry Laboratory, Department of Pharmacology and Molecular Sciences, Johns Hopkins University School of Medicine, 725 North Wolfe Street, Baltimore, MD 21205, USA

Received 1 August 2004; accepted 24 September 2004
Available online 5 November 2004

Abstract

The curved-field reflectron (CFR), developed initially to improve focusing of product ions in a dual reflectron tandem time-of-flight (RTOF/RTOF) mass spectrometer, has been used for several years in single analyzer instruments for the focusing of ions produced by post-source decay (PSD) without stepping the reflectron voltage. More recently, the addition of a collision chamber to a commercial instrument that incorporates the CFR enables both PSD and collision-induced dissociation (CID) mass spectra to be obtained in a tandem instrument without decelerating the primary ions or reaccelerating product ions to accommodate the limited energy bandwidth of the reflectron. In the PSD or laser-induced dissociation (LID) mode, i.e., without a collision gas, nearly complete b- and y-series ions are observed, which is illustrated here in the MS/MS spectra of peptides obtained in the determination of the lysine acetylation sites in a histone acetyl transferase (HAT) protein. Addition of the collision gas produces similar mass spectra, though higher collision gas pressure increases the intensities of lower mass and internal fragments, both of which appear to result from multiple collisions. In addition N-terminal sulfonation of the peptides obtained from tryptic digests produces exclusive y-series ions in the product ion mass.

Keywords: Tandem; TOF/TOF; Time-of-flight; Sulfonation

1. Introduction

In 1993, we introduced a tandem time-of-flight mass spectrometer with two dual-stage reflectron mass analyzers separated by a collision cell [1]. In the instrument shown in Fig. 1, ion activation was carried out by introducing the collision gas through a pulsed valve, timed so that the peak pressure occurred as the ions passed through the collision chamber. The use of a pulsed valve enabled very high attenuation (up to 100%) in the collision chamber, while maintaining high vacuum in the mass analyzer without the need for differential pumping. Because there was no deceleration of ions before entering the collision region, laboratory collision energies were 5 keV, defined by an ion accelerating voltage of 5 kV.

When ions fragment after leaving the ion source, they maintain the same velocity as the precursor ion (if there are no accelerating or retarding fields) but have kinetic energies:

$$E_2 = \frac{m_2}{m_1} E_1$$

where m_1 and E_1 are the mass and kinetic energy of the precursor ion, respectively, and m_2 and E_2 are the mass and kinetic energy of the product ion, respectively. Product ion energies, thus, cover a very wide range that is proportional to their masses and generally cannot be focused by the limited bandwidth of most reflectrons. In addition, in a dual-stage reflectron the kinetic energy for most of the product ion mass range is insufficient to enable the ions to penetrate the second stage, where the major focusing and time-dispersion

☆ Presented in a Symposium on *Mass Spectrometry of Biopolymers* at the ACS National Meeting in Anaheim, CA, 2004.

* Corresponding author. Tel.: +1 410 9553022; fax: +1 410 9553420.
E-mail address: rcotter@jhmi.edu (R.J. Cotter).

1387-3806/$ – see front matter © 2004 Elsevier B.V. All rights reserved.
doi:10.1016/j.ijms.2004.09.022

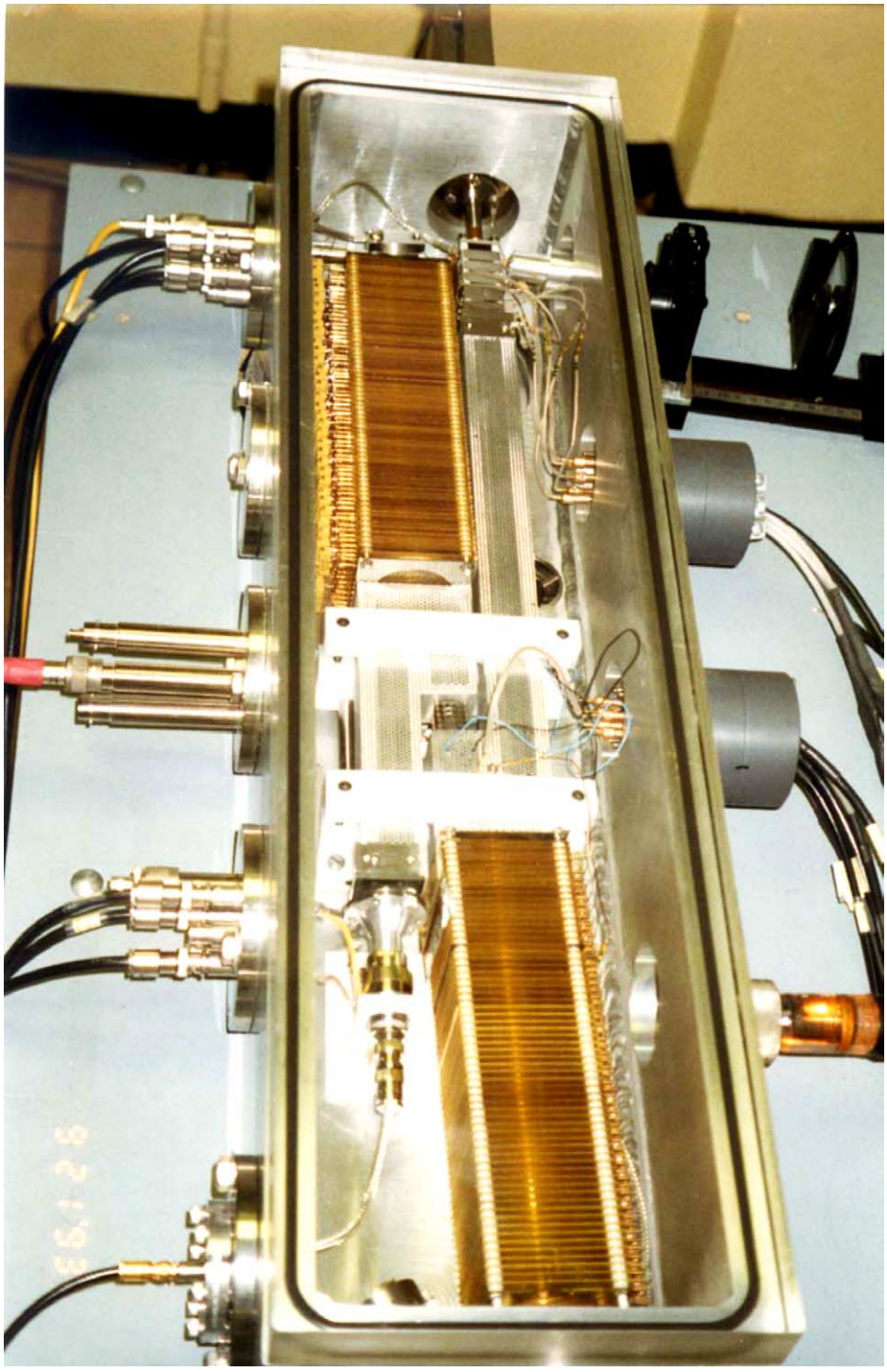

Fig. 1. Tandem time-of-flight (TOF/TOF) mass spectrometer shown here with a single stage reflectron as the first mass analyzer, a collision region with a pulsed gas valve, and a curved-field reflectron as the second mass analyzer. In the first mass analyser, $L_2 < L_1$ but $L_1 + L_2 = 4d$, where d is the average penetration depth of the reflectron. In the second mass analyzer, the total drift length $L_1 + L_2$ is shorter corresponding to the shorter focal length of the curved-field reflectron. The direct insertion probe and ionization region is shown in the upper right part of the vacuum chamber. Ions are formed by matrix-assisted laser desorption/ionization (MALDI) and extracted promptly from a two-stage source with an accelerating voltage of 5 kV.

occurs. Thus, ions with masses below about 90–95% of the precursor mass are recorded as a single unresolved peak. For that reason, our second version of the tandem time-of-flight mass spectrometer utilized two single stage reflectrons [2] for which the product ions (though not all resolved) are nonetheless dispersed along a linear mass scale:

$$t_2 = t_a + \left(\frac{m_1}{2\,\mathrm{eV}}\right)^{1/2}\left[L_1 + L_2 + 4\frac{m_2}{m_1}d\right]$$

where t_2 is the flight time of the product ion; t_a, the flight time of the precursor ion in the first mass analyser; L_1 and L_2, the drift lengths in the second mass analyzer before and after the reflectron; and d, the average penetration depth of the ions in the second reflectron.

2. Non-linear reflectrons

The "ideal" reflectron is one in which the equipotential lines along the central axis follow a square root law, that is a quadratic reflectron [3]. The property of this reflectron is that the flight time is independent of kinetic energy to infinite order. Thus, the flight time of a product ion in an instrument incorporating a quadratic reflectron as the second mass analyzer would be [4];

$$t_2 = t_a + \pi\left(\frac{m_2}{2ea}\right)^{1/2}$$

where t_a is again the flight time of the precursor ion in the first mass analyser; a, the slope of the quadratic field defined by $V = ax^2$, and x, the distance into the reflectron from its entrance. Note that the flight times in the second mass analyzer do not depend upon the mass m_1 of the precursor ions or the portion of their kinetic energy carried by the product ions. However, while attractive as the second mass analyzer in a tandem instrument, quadratic reflectrons do in fact have some drawbacks. In particular, the shape of the field in the off-axis direction, defined by imposing the quadratic potential along the centerline, results in wide dispersion of the incoming (and outgoing) ion beam such that the transmission becomes poor for an ion having a transverse component of initial velocity, entering at an angle or off-axis. In addition, the quadratic reflectron focuses ions from a point at its entrance, i.e., there are no drift lengths L_1 and L_2. Upon activation, ions may continue to fragment after leaving the collision chamber so that a reflectron that accommodates an additional drift length may be desirable.

Another alternative is to decelerate the precursor ions, generally by raising the potential of the collision cell, form product ions with a much-reduced range of kinetic energies, and then reaccelerate these ions as they enter the second mass analyzer where they can be more easily focused by a single or dual-stage reflectron. A disadvantage of this approach is that it decreases the available collision energy, but this was an appropriate and effective scheme for the photodissociation two-reflectron tandem mass spectrometer designed (also in 1993) by Enke and co-workers [5]. An additional problem is that product ions formed after reacceleration will have different flight times than those formed in the collision chamber. In our tandem mass spectrometer it was indeed possible to float the collision cell to reduce the range of product ion energies but in this configuration, we observed *artifact peaks* from ions formed within the second mass analyzer.

The problem of focusing product ions led in our laboratory to the development of the so-called curved-field reflectron (CFR) [6]. This non-linear reflectron produced a more uniform focusing across the product ion mass (and energy) range, using a field defined by voltages on the retarding lenses that followed the equation for the arc of a circle. In addition, because this field was considerably closer to the linear (constant field) case than the quadratic reflectron, ion transmission was not appreciably reduced. Also, because ions are not retarded or reaccelerated, product ions formed in the linear regions before and after the collision cell will have the same flight times as those which fragment promptly upon collision.

The performance of this instrument is shown in the collision-induced dissociation (CID) mass spectra of the fullerenes C_{60} shown in Fig. 2. Addition of helium gas enabled attenuation of 20%, 80% and 98% of the molecular ion beam, resulting in multiple collisions that shift the fragments observed to lower mass [7]. At the highest attenuation (98%) the large number of collisions required to produce the lowest mass fragments also reduces their mass resolution.

3. The curved-field reflectron and post-source decay

One difficulty with this configuration was the occurrence of metastable (laser-induced) fragmentation in the first mass analyzer. Because these fragment ions pass through the first reflectron they do not arrive at the mass selection gate and collision cell at the same time as their precursors, and are therefore not recorded in the product ion mass spectrum. Since the amount of such metastable fragmentation was not insignificant, this somewhat reduced the effectiveness of this (two reflectron) approach to tandem TOF design.

At the same time, Spengler and co-workers [8] demonstrated that one could exploit this post-source decay (PSD) for peptide sequencing in a single reflectron instrument. Again, the problem was to focus the wide kinetic energy range of the product ions in a reflectron, although the use of a single mass analyzer precluded the use of deceleration and reacceleration as would be possible between mass analyzers in a tandem instrument. Thus, the practice of stepping the reflectron voltage to accommodate successive mass (energy) segments became an integral part of the PSD method. This method is illustrated schematically in Fig. 3, which shows that the range of kinetic energies of product ions exceeds the bandwidth of the reflectron. By decrementing the reflectron voltage V_R from its initial value (optimized for molecular ions), different regions of the product ion spectrum can be brought into focus. Since separate spectra are acquired for

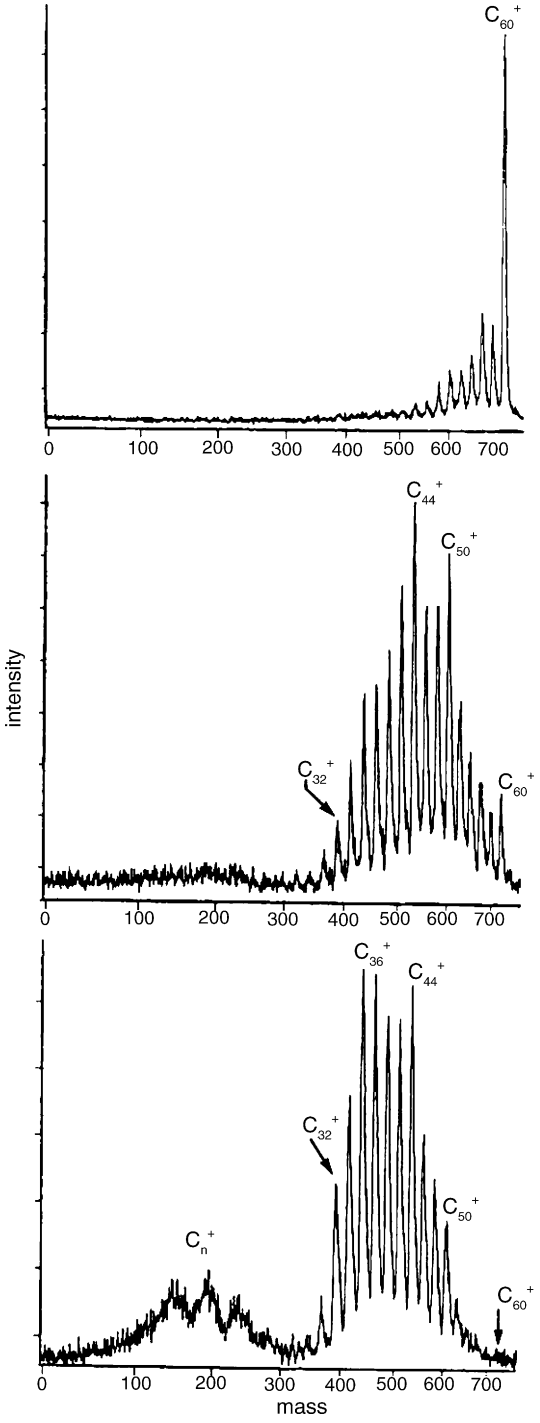

Fig. 2. Collision-induced dissociation (CID) mass spectra of buckminsterfullerene C_{60} with helium collision gas adjusted for 20%, 80% and 98% attenuation of the ion at *m*/*z* 720. (Reprinted with permission from [7]).

each setting of V_R, the focused segments of these spectra are then *stitched* together to form a final spectrum. In addition to the need for acquiring more spectra and the time involved in doing so, more samples may be required and sensitivity may vary for each of the spectral segments.

The curved-field reflectron provided a means for recording PSD spectra in a single acquisition without stepping the reflectron voltage [9,10]. While the CFR cannot provide infinite order focusing throughout the mass range, as would be the case for a quadratic reflectron, the effective bandwidth (Fig. 4) covers most of the mass and energy range of the product ions. This has important implications for the analyses of amino acid sequence and post-translational modifications of peptides obtained from tryptic and other enzymatic digests. Because the spectral acquisition time for obtaining product ion mass spectra is effectively the same as for normal MS spectra (when stepping is not required), the acquisition of such spectra for every peptide observed from the digest becomes practical.

4. Lysine acetylation in histone acetyl transferase

Histone acetyl transferases (HAT) covalently modify histones and other substrates by transferring acetyl groups from acetyl-CoA to the ε-amino groups of specific lysine residues. Reversible acetylation and deacetylation of histones and other DNA-binding proteins affects their functions and has been established to be a key mechanism in regulating gene transcription. In addition, the acetylation of non-histone proteins is also involved in other functions including the regulation of protein-protein interactions and protein stability. Using matrix-assisted laser desorption/ionization (MALDI) and PSD analysis, we recently determined the acetylation sites within a purified recombinant HAT domain of p300 protein [11], a cellular 300 kDa protein identified as a nuclear protein that binds to the adenoviral E1A oncoprotein. In characterizing the multiple sites for lysine acetylation, we obtained product ion mass spectra of 63 of 70 peptides observed in the mass spectra of the tryptic digest (Table 1). Twenty-eight of these peptides were acetylated at one or more sites, with most of the sites within a nested domain from residues 266 to 299. Fig. 5 shows the product ion mass spectrum of a peptide 266–284 with a single acetylation site. Generally, the product ion mass spectra of the non-acetylated tryptic peptides contained complete or nearly complete b- and y-series ions [12]. In contrast the acetylated peptides produced predominant b-series and some c-series ions. Note also in Fig. 5 that cleavages adjacent to aspartic acid residues (b_{12} and b_{17}) are more pronounced. This is also the case for the peptides containing 2 and 4 lysine acetylation sites shown in Figs. 6 and 7. These mass spectra were all obtained on a Kratos (Manchester, UK) AXIMA-CFR mass spectrometer.

5. The new tandem (TOF/TOF) mass spectrometers

It has been common to cite the new generation of tandem (TOF/TOF) time-of-flight mass spectrometers as alternatives to PSD. To some degree this is an inappropriate comparison since PSD describes primarily a method of ion activation that may include the imparting of internal energy directly during

Table 1
Peptides from the tryptic digest of histone acetyl transferase analyzed by PSD

No.	Peptide position	MH + mass (measured)	MH + mass (calculated)	Peptide sequence
1	2–10	1073.0	1073.1	GSSHHHHHH
2	2–14	1433.3	1433.4	GSSHHHHHHSSGE
3	2–16	1661.7	1660.7	GSSHHHHHHSSGENL
4	2–17	1824.0	1823.9	GSSHHHHHHSSGENLY
5	2–18	1971.7	1971.0	GSSHHHHHHSSGENLYF
6	16–28	1497.7	1498.7	LYFGGHKENKFSA
7	30–35	729.8	729.4	RLPSTR
8	36–43	951.4	949.5	LGTFLENR
9	44–49	754.4	763.4	VNDFLR
10	50–55	780.1	780.5	RQNHPE
11	50–62	1508.9	1508.9	RQNHPESGEVTVR
12	51–62	1363.9	1362.7	QNHPESGEVTVR
13	61–70	1338.9	1340.5	VRWHASDKTVE
14	70–78	989.4	989.2	TVEVKPGMK
15	70–80	1260.5	1258.	TVEVK_{Ac}PGMKAR
16	81–94	1634.7	1634.7	FVDSGEMAESFPYR
17	97–129	3732.3	3732.7	ALFAFEEIDGVDLCFFGMHQEYGSDCPPPNQR
18	131–141	1344.2	1343.5	VYISYLDSVHF
19	131–145	1872.5	1872.0	VYISYLDSVHFFRPK
20	136–145	1247.8	1246.5	LDSVHFFRPK
21	141–145	695.0	694.9	FFRPK
22	149–164	1912.3	1912.0	TAVYHEILIGYLEYVK
23	155–163	1084.3	1083.3	ILIGYLEYV
24	157–164	985.2	985.2	IGYLEYV
25	166–194	3287.5	3286.6	LGYTTGHIWACPPSEGDDYIFHCHPPDQK
26	169–194	2952.4	2952.2	TTGHIWACPPSEGDDYIFHCHPPDQK
27	186–197	1448.5	1447.1	FHCHPPDQKIPK
28	196–206	1588.6	1586.9	IPKPKRLQEWYK
29	200–206	1022.6	1022.5	RLQEWYK
30	201–206	867.0	867.0	LQEWYK
31	201–216	2027.4	2025.1	LQEWYKKMLDKAVSER
32	205–213	1139.9	1138.4	YKKMLDK_{Ac}AV
33	212–226	1823.9	1820.0	AVSERIVHDYKDIFK
34	217–222	775.6	774.4	IVHDYK
35	233–256	2856.5	2856.2	LTSAK_{Ac}ELPYFEGDFWPNVLEESIK
36	238–256	2313.0	2313.1	ELPYFEGDFWPNVLEESIK
37	248–256	1029.2	1029.2	PNVLEESIK
38	257–265	1191.2	1190.5	ELEQEEEER
39	266–281	1838.2	1836.9	KREENTSNESTDVTK_{Ac}G
40	266–284	2168.6	2168.2	KREENTSNESTDVTK_{Ac}GDSK
41	266–285	2324.3	2324.4	KREENTSNESTDVTK_{Ac}GDSK_{Ac}N
42	266–286	2396.9	2395.5	KREENTSNESTDVTK_{Ac}GDSK_{Ac}NA
43	266–287	2566.6	2565.7	KREENTSNESTDVTK_{Ac}GDSK_{Ac}NAK_{Ac}
44	266–288	2694.9	2693.8	KREENTSNESTDVTK_{Ac}GDSK_{Ac}NAK_{Ac}K
45	266–289	2864.4	2864.1	KREENTSNESTDVTK_{Ac}GDSK_{Ac}NAK_{Ac}K$_{Ac}$K
46	266–289	2907.9	2906.1	KREENTSNESTDVTK_{Ac}GDSK_{Ac}NAK_{Ac}K$_{Ac}$K$_{Ac}$
47	266–290	3020.7	3020.2	KREENTSNESTDVTK_{Ac}GDSK_{Ac}NAK_{Ac}K$_{Ac}$K$_{Ac}$N
48	266–291	3135.2	3134.9	KREENTSNESTDVTK_{Ac}GDSK_{Ac}NAK_{Ac}K$_{Ac}$K$_{Ac}$NN
49	266–292	3263.2	3262.5	KREENTSNESTDVTK_{Ac}GDSK_{Ac}NAK_{Ac}K$_{Ac}$K$_{Ac}$NNK
50	266–292	3305.2	3304.5	KREENTSNESTDVTK_{Ac}GDSK_{Ac}NAK_{Ac}K$_{Ac}$K$_{Ac}$NNK$_{Ac}$
51	266–293	3433.3	3432.7	KREENTSNESTDVTK_{Ac}GDSK_{Ac}NAK_{Ac}K$_{Ac}$K$_{Ac}$NNK$_{Ac}$K
52	266–293	3475.5	3474.7	KREENTSNESTDVTK_{Ac}GDSK_{Ac}NAK_{Ac}K$_{Ac}$K$_{Ac}$NNK$_{Ac}$K$_{Ac}$
53	266–294	3576.2	3575.8	KREENTSNESTDVTK_{Ac}GDSK_{Ac}NAK_{Ac}K$_{Ac}$K$_{Ac}$NNK$_{Ac}$K$_{Ac}$T
54	266–295	3663.4	3662.9	KREENTSNESTDVTK_{Ac}GDSK_{Ac}NAK_{Ac}K$_{Ac}$K$_{Ac}$NNK$_{Ac}$K$_{Ac}$TS
55	266–296	3791.9	3791.1	KREENTSNESTDVTK_{Ac}GDSK_{Ac}NAK_{Ac}K$_{Ac}$K$_{Ac}$NNK$_{Ac}$K$_{Ac}$TSK
56	266–296	3834.2	3833.1	KREENTSNESTDVTK_{Ac}GDSK_{Ac}NAK_{Ac}K$_{Ac}$K$_{Ac}$NNK$_{Ac}$K$_{Ac}$TSK$_{Ac}$
57	266–297	3947.5	3947.2	KREENTSNESTDVTK_{Ac}GDSK_{Ac}NAK_{Ac}K$_{Ac}$K$_{Ac}$NNK$_{Ac}$K$_{Ac}$TSK$_{Ac}$N
58	266–298	4077.4	4075.4	KREENTSNESTDVTK_{Ac}GDSK_{Ac}NAK_{Ac}K$_{Ac}$K$_{Ac}$NNK$_{Ac}$K$_{Ac}$TSK$_{Ac}$NK
59	266–298	4118.3	4117.4	KREENTSNESTDVTK_{Ac}GDSK_{Ac}NAK_{Ac}K$_{Ac}$K$_{Ac}$NNK$_{Ac}$K$_{Ac}$TSK$_{Ac}$NK$_{Ac}$
60	266–299	4205.1	4204.5	KREENTSNESTDVTK_{Ac}GDSK_{Ac}NAK_{Ac}K$_{Ac}$K$_{Ac}$NNK$_{Ac}$K$_{Ac}$TSK$_{Ac}$NK$_{Ac}$S
61	267–289	2736.8	2735.9	REENTSNESTDVTK_{Ac}GDSK_{Ac}NAK_{Ac}K$_{Ac}$K$_{Ac}$
62	285–293	1114.5	1115.3	NAKKKNNK$_{Ac}$K

Table 1 (*Continued*)

No.	Peptide position	MH + mass (measured)	MH + mass (calculated)	Peptide sequence
63	308–321	1515.7	1515.7	KPGMPNVSNDLSQK
64	308–328	2351.1	2362.7	KPGMPNVSNDLSQKLYATMEK
65	331–337	910.2	909.5	EVFFVIR
66	338–365	2872.9	2872.4	LIAGPAANSLPPIVDPDPLIPCDLMDGR
67	366–373	907.3	906.5	DAFLTLAR
68	374–383	1232.9	1231.6	DKHLEFSSLR
69	374–383	1275.5	1274.4	DK_{Ac}HLEFSSLR
70	376–383	989.6	988.6	HLEFSSLR

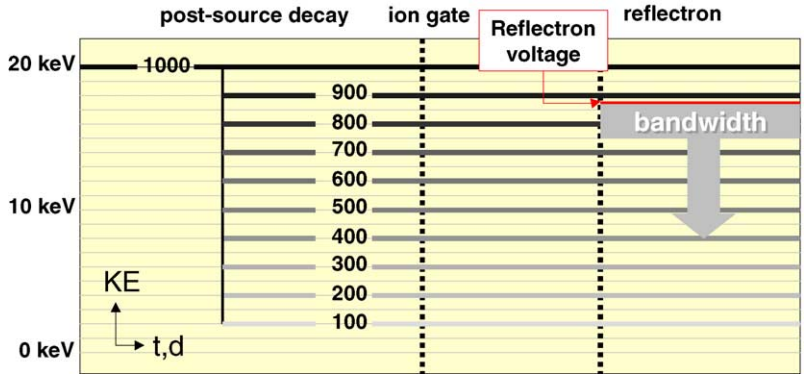

Fig. 3. Diagram of the kinetic energies of molecular and product ions as these ions traverse a reflectron mass spectrometer. Molecular ions of *m*/*z* 1000 are extracted from the source with energies of 20 kev, while fragment ions formed by PSD carry energies proportional to their masses. These are not all focused by single or dual-stage reflectrons. In particular, the single stage reflectron is designed such that $L_1 + L_2 = 4d$, where d is the penetration depth for optimal focusing. The potential at that depth V_d is related to the voltage on the back of the reflectron: $V_d = V_R(d/d_0)$, where V_R is the reflectron voltage and d_0 is the full length of the reflectron. When $V_d = V_{acc}$ (the accelerating voltage), then precursor ions are focused. When $V_d = 18$ kV, then (in this example) ions with *m*/*z* 900 are in optimal focus. Thus, lowering the reflectron voltage in steps produces spectra in which different mass regions are in focus.

the MALDI process, metastable dissociation after ions leave the source and some collision-induced dissociation with background molecules or with gases that are added intentionally. If, however, the term PSD has come to assume a method for product ion focusing that must necessarily include stepping the reflectron voltage, then indeed the new TOF/TOF instruments accomplish that focusing differently. This, of course, was not the case when the curved-field reflectron was used.

Perhaps the most obvious distinction between tandem TOF mass spectrometers and TOF instruments used in the PSD mode is that in the tandem there are in fact two mass analyzers separated by a collision chamber. The collision chamber is of course intended to provide the opportunity for collision-induced dissociation, but in fact many MS/MS spectra are obtained on tandem TOF instruments with *no collision gas*. While the processes then leading to the observed fragmentation are identical to those that are utilized

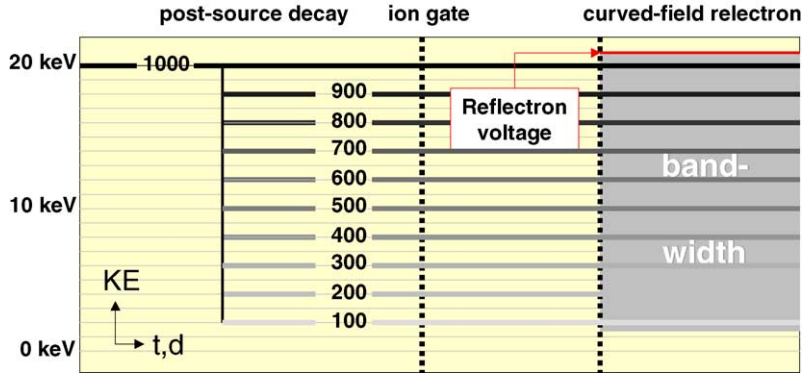

Fig. 4. Kinetic energy diagram of molecular and product (PSD) ions in a curved-field reflectron TOF mass spectrometer. Because of the higher bandwidth of this reflectron, a wider range of product ions can be focused using a fixed reflectron voltage.

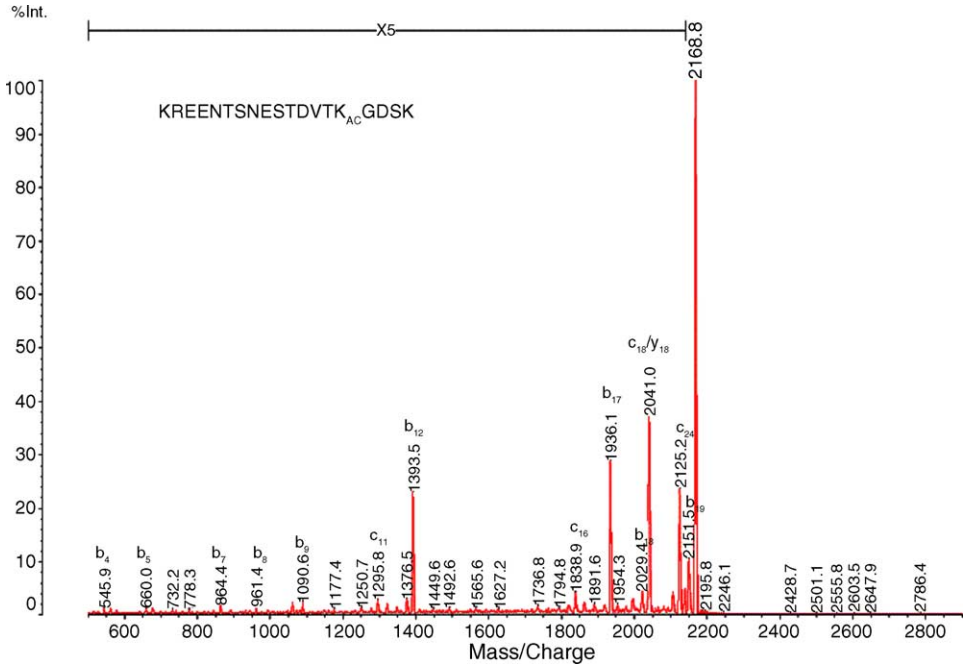

Fig. 5. Product ion mass spectrum of a tryptic peptide from histone acetyl transferase (HAT) that contains a single acetylation site. Both b- and c-series ions appear in the mass spectrum, and prominent fragmentation occurs at the two aspartic acid residues. (Reprinted with permission from [12]).

in the PSD method, it has also been common to refer to this as laser-induced dissociation (LID) specifying the origins of activation as arising from the MALDI process. Thus, the major property of a tandem instrument is the focusing of ions in time at a point that distinguishes the two mass analyzers. This permits optimal resolution for precursor mass selection, which was often not the case with earlier PSD mass spectrometers. In that sense, the AXIMA CFR instrument used here is in fact a tandem instrument, though without a collision chamber, and this then motivated the modifications to that instrument that are described below to permit both laser-induced and collision-induced dissociation.

Based upon our initial experience with the reflectron tandem time-of-flight (RTOF/RTOF) [6], it has been our belief that post-source fragmentation is a practically unavoidable result of the MALDI ionization process, and that an important

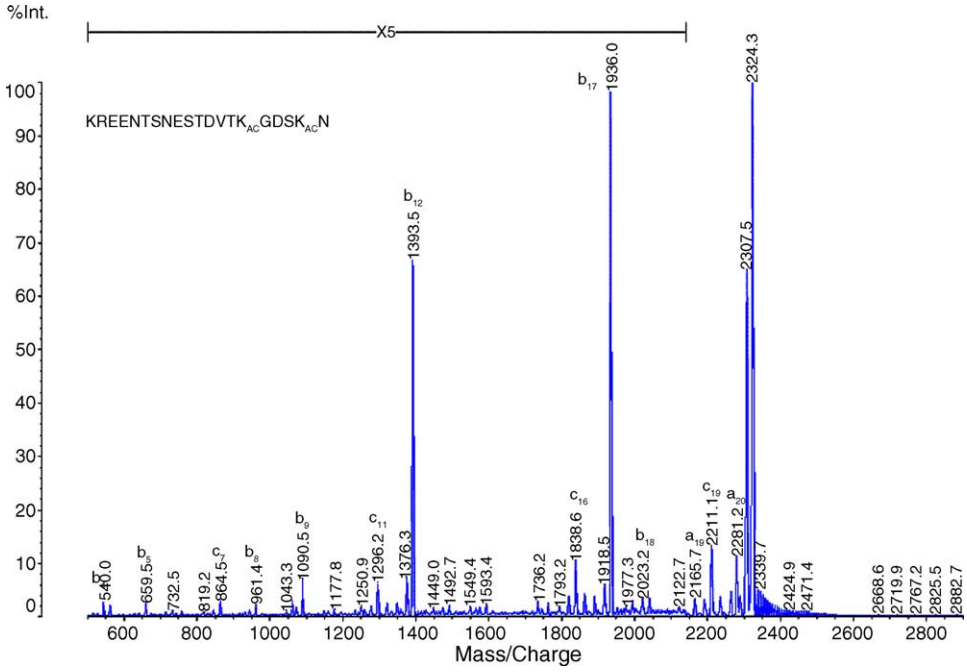

Fig. 6. Product ion mass spectrum of a tryptic peptide from histone acetyl transferase (HAT) with two acetylation sites. (Reprinted with permission from [12]).

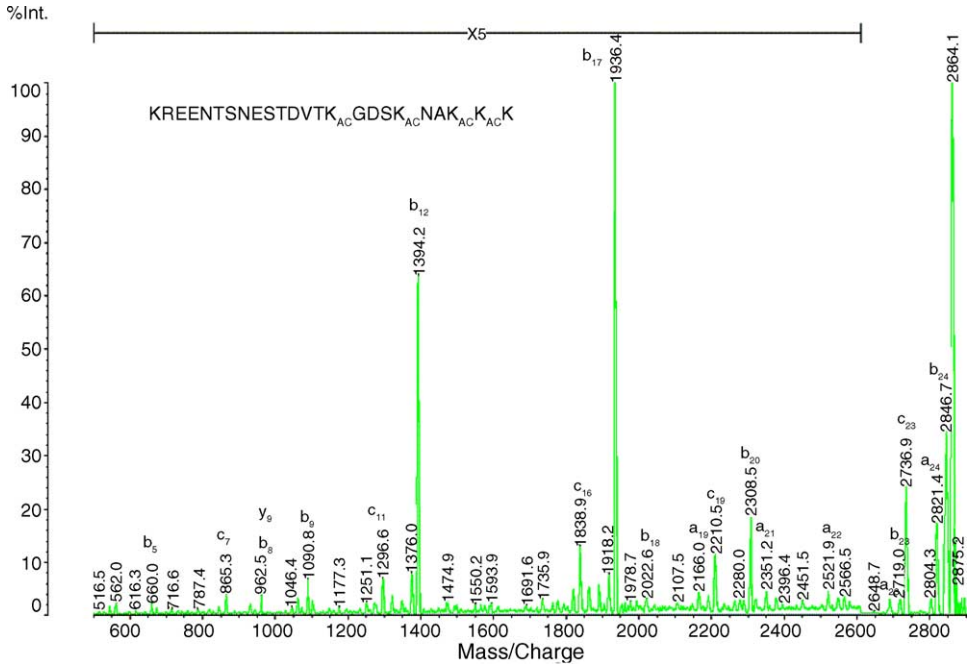

Fig. 7. Product ion mass spectrum of a tryptic peptide from histone acetyl transferase (HAT) with four acetylated lysine residues. (Reprinted with permission from [12]).

aspect of TOF/TOF design is related to how that fragmentation is to be handled and indeed to be utilized. Secondly, in developing a TOF/TOF instrument in our own laboratory, we have intended to use the highest possible collision energy E_{lab}, based (in the laboratory frame) upon the full kinetic energy of ions accelerated from the source. For a large precursor ion of mass m_p striking a light target m_n the relative energy E_{rel}

$$E_{rel} = \frac{m_n}{m_n + m_p} E_{lab}$$

is very small unless the laboratory energy is quite large. Table 2 gives some examples of the relative energies for several peptides, laboratory energies and target gases.

6. "Second source" approaches

In all of the instruments described below, the first mass analyzer is a *linear* TOF with ions brought to a focal point using pulsed or time-delayed extraction [13–15]. In one approach that is shown in Fig. 8a, precursor ions are decelerated prior to entering the collision chamber to laboratory kinetic energies between 1 and 2 keV [16]. This approach is similar to that described by Enke and co-workers [5] for a dual reflectron instrument except that the product ions are then reaccelerated by pulsed extraction from what is effectively a second source. Slowing the precursor ions down does reduce the collision energies, but in addition (and as shown in Fig. 8b) those fragment ions that have formed by post-source process occurring before the precursor ions enter the collision chamber do not enter the collision chamber and do not contribute to the mass spectrum. Similarly, product ions that are formed after reacceleration have considerably different kinetic energies that those formed in the collision cell. They therefore will have different flight times and would not contribute constructively to the final spectrum; rather they would produce *artifact peaks*. The lower kinetic energies of these ions allow them to be removed by a deflection system or *metastable suppressor*.

In another approach, shown schematically in Fig. 9a, ions enter the collision chamber with full 8 keV kinetic energy provided by the ion source [17]. Because the precursor ions are not decelerated prior to entering the collision chamber, any fragment ions formed after the source will have the same velocities as their precursors, will be mass selected along with their precursors and will enter the collision chamber at the same time where they will be joined by additional fragment ions formed by collision. Thus, all of the ions formed by metastable (or laser-induced) and CID processes will be focused in and will contribute to the product ion mass spectrum from the same mass-selected precursor (Fig. 9b). In addition, all of the fragment ions along with their precursor are moving at the same velocity before entering the reflectron used as the second mass analyzer. Therefore, they can be simultaneously post-accelerated by abruptly raising the potential of the collision or other *lift* cell. Fragment ions formed after that step will, of course, not be focused or be recorded at the same time and would again appear as artifacts in the spectrum. In this scheme, they are removed by gating the remaining precursor ions that leave the lift cell.

Table 2
Collision energies for several peptides when the laboratory energies are 1, 8 and 20 keV, corresponding to the instruments described above and in [16] [17] and [18], respectively, using helium and argon as collision gases

Protein	Molecular weight	1 (keV) (eV)	8 (keV) (eV)	20 (keV) (eV)
(a) with helium collision gas				
Substance P	1348	2.97	23.7	59.4
Ubiquitin	8566	0.47	3.7	9.3
Cytochrome C	12,328	0.32	2.6	6.5
C fragment of tetanus toxin	51,819	0.08	0.6	1.4
Bovine serum albumin	66,430	0.06	0.5	1.2
(b) with argon collision gas				
Substance P	1348	29.7	237	594
Ubiquitin	8566	4.7	37	93
Cytochrome C	12,328	3.2	26	65
C fragment of tetanus toxin	51,819	0.8	6	15
Bovine serum albumin	66,430	0.6	5	12

7. Neither lifting nor stepping

We, recently, modified a Kratos (Manchester, UK) AXIMA CFR mass spectrometer with the addition of a collision chamber placed between the ionization source and the mass selection gate [19]. The collision chamber was constructed from a 1.13 in. long, 0.2 in. i.d. stainless steel cylinder placed in the ion beam. The collision gas enters at the center of the cylinder through a long (2 m) 0.070 mm i.d. glass capillary tube at a flow rate of 0–1 ml/min. Because of the limited conductance of the cylinder it is possible to achieve relatively high pressure in the center of the collision region, while maintaining high vacuum in the surrounding chamber. Because this arrangement does not permit us to measure the pressure in the cylinder directly, we have generally monitored both the backing pressure at the gas cylinder regulator and the ambient

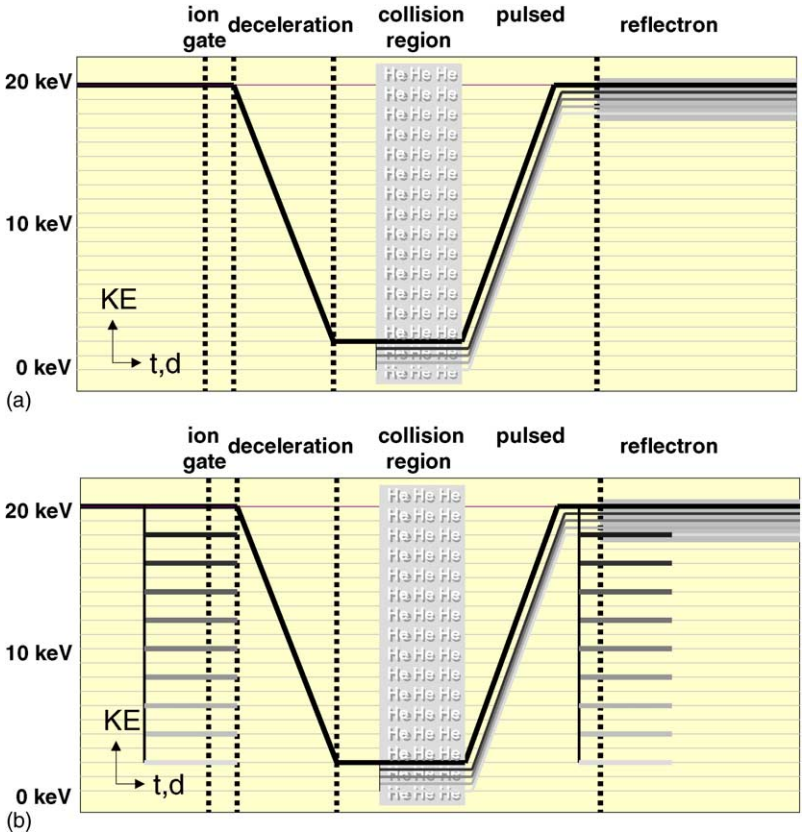

Fig. 8. (a) Kinetic energy diagram for a tandem time-of-flight approach in which the precursor ions are first decelerated from the source energy of 20 keV to 1–2 keV before entering the collision chamber, and the product ions are then reaccelerated into the second mass spectrometer using a pulsed extraction "second source". (b) Kinetic energy diagram for this approach showing the energies of product ions formed by metastable dissociation occurring in the first mass analyzer before deceleration and after reacceleration into the second mass analyzer.

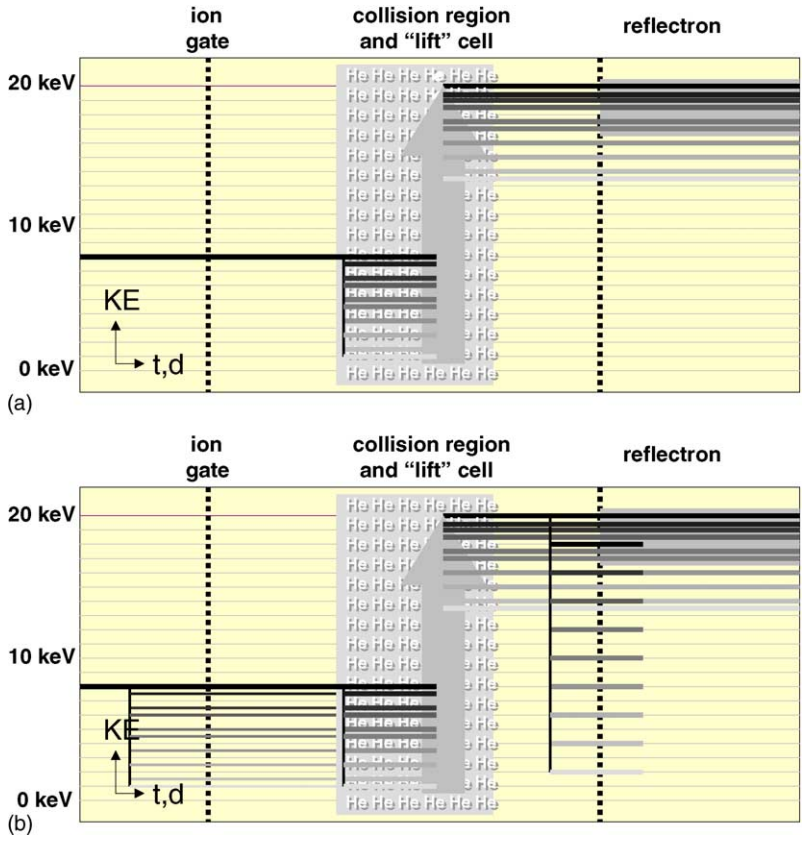

Fig. 9. (a) Kinetic energy diagram for a tandem time-of-flight approach in which the precursor ions are not decelerated in the first mass analyzer and enter the collision chamber at 8 keV. Mass-selected precursors and their products have the same velocities and enter a "lift cell" at the same time, at which time the potential of the cell is raised. (b) Kinetic energy diagram for this approach showing the energies of ions formed my metastable dissociation before the collision chamber and after leaving the lift cell.

vacuum as the means to provide reproducible or comparative collision conditions.

Fig. 10a shows the kinetic energy diagram for ions dissociated in the collision chamber when this instrument with a curved-field reflectron is used. This is in fact the same as that shown in Fig. 4 for the analysis of PSD ions, as in fact the means for focusing all product ions is identical in this instrument. Fig. 10b illustrates that point by showing that the same ions formed by PSD (metastable, laser-induced and/or opportunistic collision) processes occurring before and after the collision chamber enter the reflectron at the same energies, at the same times and are focused in the same manner.

Fig. 11 shows the CID mass spectra of buckminsterfullerene (C_{60}) obtained at different collision gas pressures monitored by the backing pressures in psi. Under the conditions used, the molecular ion undergoes very little metastable fragmentation when no helium gas is present (Fig. 10a). Fragmentation increases with increasing helium gas pressure, and in addition produces more fragment ions of lower mass. Fig. 12 monitors three of the ions, the molecular ion at *m/z* 720 and the fragments at *m/z* 600 and 180. The molecular ion shows considerable attenuation at the higher helium gas pressures with a collision cross section of 4×10^{-15} cm^2 that would include losses of this ion through both scattering and fragmentation. In this experiment the formation of the fragment at *m/z* 600 increases, but the intensity of this ion reaches a maximum and then decreases presumably as the result of additional collisions that also include scattering and the formation of lower mass fragments. The latter is confirmed by the formation of lower mass fragments at *m/z* 180 whose intensities reach their maximum at higher gas pressures. Thus, this arrangement of the collision chamber provides sufficient pressure to enable multiple collisions, though the greatly improved mass resolution of low mass fragments as compared with those in Fig. 2 suggests that these are limited to far fewer collisions than in the earlier instrument. This indeed might be expected since the current instrument provides 20 keV (laboratory frame) collision energies, while the earlier instrument used 5 keV energies.

Fig. 13 shows the 20 keV CID mass spectra of substance P at two different. Pressures of helium gas. Again, at higher collision gas pressures there is an increase in the lower mass ions, suggesting that these may be formed by additional collisions. While the fragment ions observed by CID are not very different from those observed by PSD processes, there is generally an increase in the number and intensity of internal ions (data not shown) suggesting that these arise from breaking a second bond on either CID or PSD fragments.

8. N-terminal sulfonation

The ability to obtain MS/MS spectra with relative ease and efficiency using the curved-field reflectron has generally motivated approaches in which all or nearly all observed peptides from a tryptic digest are subjected to laser or collision-induced dissociation. The interpretation of these MS/MS spectra in order to determine amino acid sequences can then be greatly simplified by derivatization of the N-terminal amino group of the precursor peptide using 4-sulfophenyl isothiocyanate (SPITC) as the derivatization reagent [19,20]. The addition of a negatively-charged group on the N-terminus effectively eliminates the formation of positively-charged N-terminal fragment ions producing nearly exclusively y-series ions. We have reported a modification to the sulfonation reaction in which the co-reagent triethylamine (TEA) is replaced with sodium bicarbonate [21]. This reagent appears to be more compatible with the requirements of the mass spectrometer and the reaction can be performed under aqueous conditions with high efficiency. Fig. 14 shows an example of an MS/MS spectrum of an N-terminal sulfonated peptide obtained on our tandem instrument using laser-induced dissociation, i.e., without the collision gas. In addition to the complete set of y-series sequence ions, there is also a major peak corresponding to the loss of 215 mass units that is characteristic of N-terminal sulfonated peptides.

9. Conclusions and future prospects

The time-of-flight mass spectrometer is actually an old concept that was first developed as a successful commercial instrument by Wiley and McLaren in 1955 [22]. The idea that this was a low mass range, low mass resolution instrument has certainly been turned around by today's high performance versions, due largely to the development of these instruments that has accompanied the introduction of matrix-assisted laser desorption/ionization [23,24] and *electrospray ionization* [25]. Perhaps more interesting is that the original commercial instruments had a very low duty cycle due to the need for scanning a time-gated detection window, a method also known as "boxcar" recording. Concurrent with the development of laser microprobes [26], laser ionization [27], IR laser desorption [28] and plasma desorption instruments [29] in the 1970s and 1980s, the availability of fast transient and time-to-digital recording devices enabled these instrument to realize their potential as multichannel recording devices, capable of recording ions of all masses simultaneously. While the introduction of the PSD technique as the "poor man's tandem" has been a most significant contribution to the development of time-of-flight mass spectrometers for protein sequencing, the need for stepping the reflectron voltage is reminiscent of the boxcar method, partially losing the multichannel advantage as it utilizes only portions

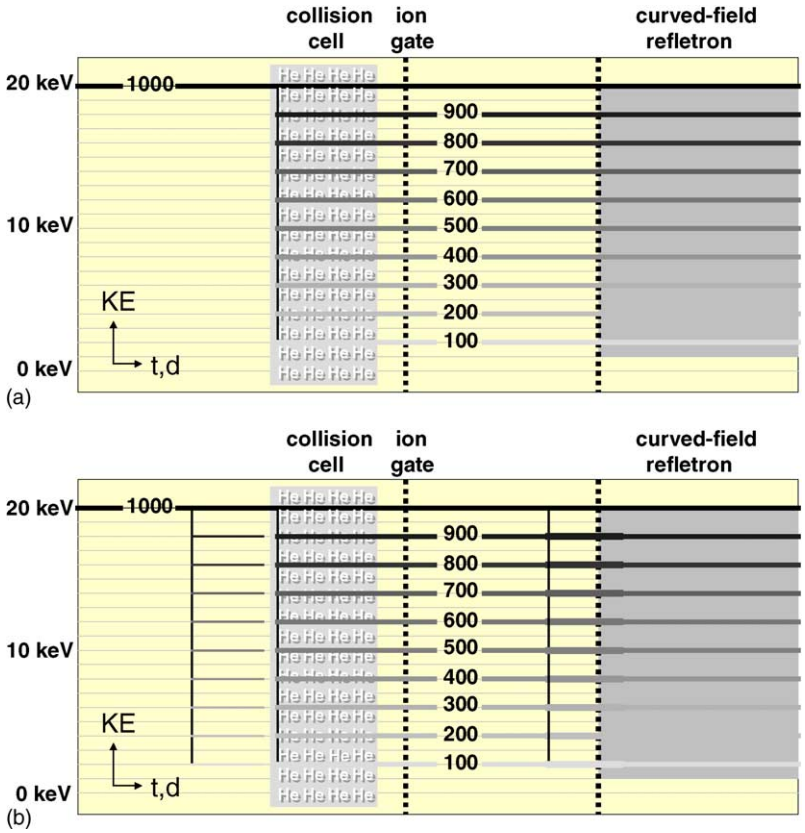

Fig. 10. (a) Kinetic energy diagram for a tandem time-of-flight approach in which ions are not decelerated or reaccelerated but are focused by a curve-field reflectron. (b) Kinetic energy diagram for this approach showing the energies for ions formed by metastable processes before and after the collision chamber.

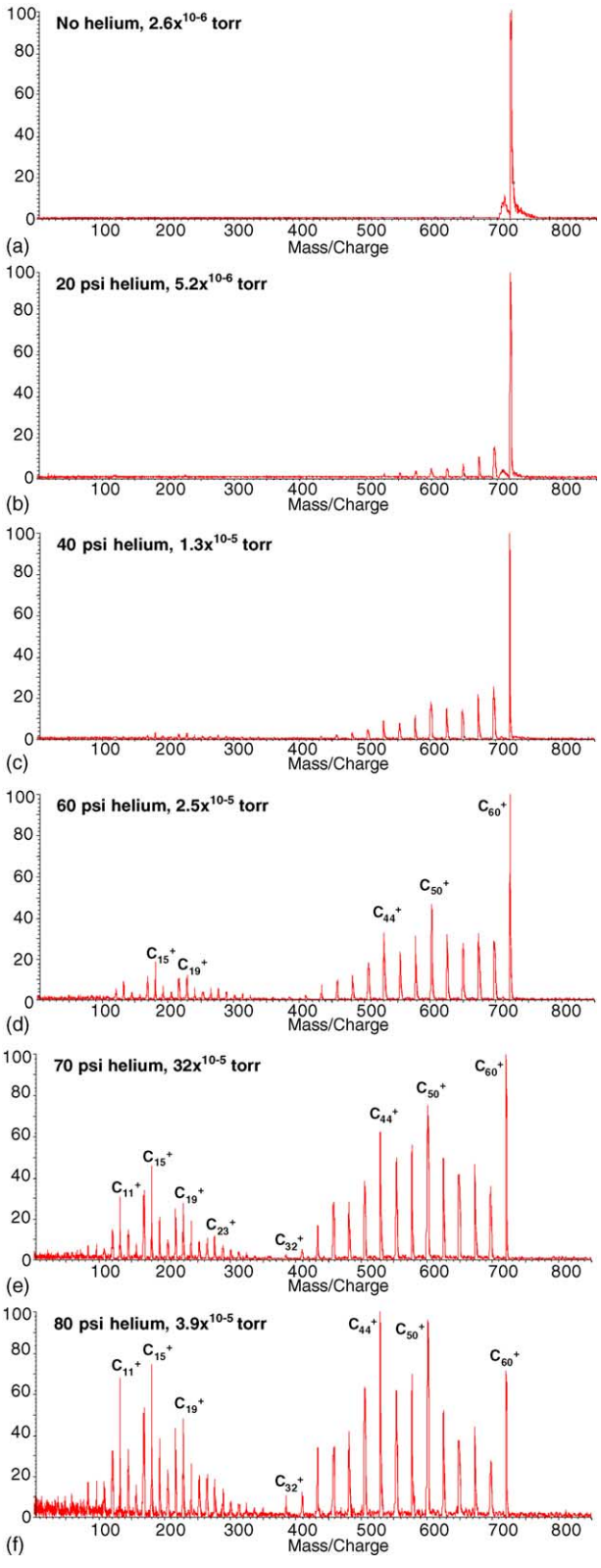

Fig. 11. Collision-induced dissociation (CID) mass spectra of buckminsterfullerene (C_{60}) as a function of increasing collision gas pressure using a curved-field reflectron tandem TOF mass spectrometer. Because the pressure inside the collision chamber is not known, the pressures applied to the gas inlet (in psi) and the analyzer background pressure (in torr) are listed. (Reprinted with permission from [18]).

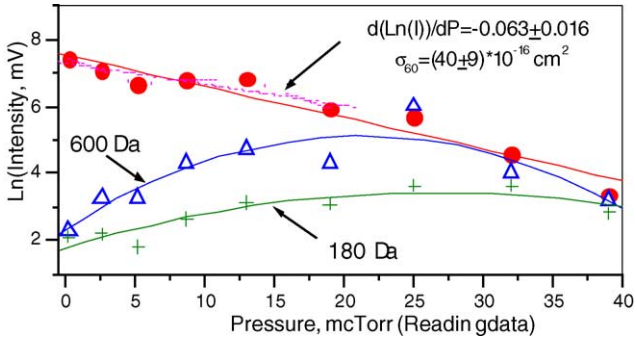

Fig. 12. Intensity vs. collision gas backing pressure (in psi) for the ions from C_{60} at *m*/*z* 720, 600 (C_{50}) and 180 (C_{15}).

of the mass range in each cycle. It is this aspect of the TOF mass spectrometer that is addressed by the development of the curved-field reflectron, and as well by the new methods for "lifting" ions that are being used in tandem TOF/TOF instruments.

Any tandem instrument is necessarily multichannel in only one dimension, i.e., in the most common *product ion* experiment, we record simultaneously only all of those ions from a single parent; and the first mass analyzer is utilized as a mass filter. While this implies that we lose all of those ions from precursors that are not being selected, it should not be necessary to lose any fragment ions from the precursor ion that has been selected. Provided that there are no retarding or accelerating voltages in the region between the source and the

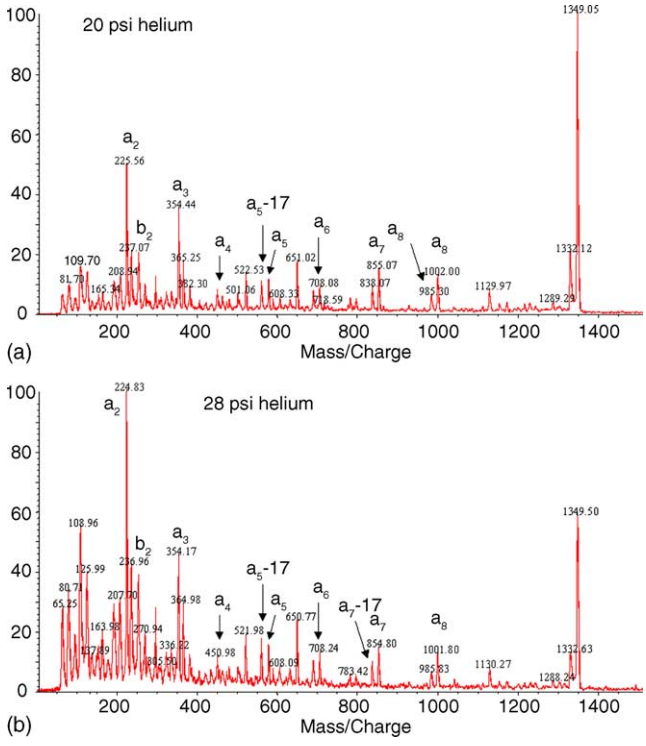

Fig. 13. CID mass spectra of substance P at two different collision gas pressures. At the high pressure there is an increase in lower mass fragment ions. (Reprinted with permission from [18]).

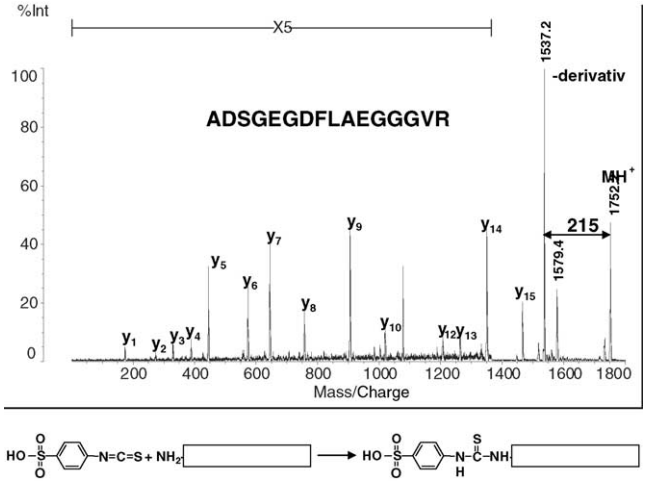

Fig. 14. Laser-induced dissociation MS/MS spectrum of an N-terminal sulfonated peptide.

reflectron, than all fragment ions formed post-source will retain the same velocities and be recorded. The curved-field reflectron addresses that issue as well, treating both metastable (laser-induced) and CID fragment ions identically.

The ability to carry out very high (laboratory) energy collisions may also be an important aspect of this approach. While MS/MS has now become common for peptide amino acid sequencing by both MALDI and electrospray it has been carried out in large part by instruments that employ low energy collisions, i.e., quadrupole ion traps, hybrid quadrupole/time-of-flight (QTOF) mass spectrometers and Fourier transform mass spectrometers (FTMS). While the distinction between what is high and low energy is sometimes unclear, an important characteristic of low energy collisions is the need to use multiple collisions that lead, ultimately, to the breaking of the weakest bond. This is also true of thermal excitation methods such as infrared multiphoton dissociation (IRMPD) [30] that may result in incomplete sequence fragmentation and/or loss of side groups characteristic of post-translational modifications. Thus, there has been considerable interest in the development of electron capture dissociation (ECD) [30,31] as an alternative to CID that will result in more random fragmentation. However, this is also a characteristic of single high-energy collisions, the so-called *charge remote fragmentation* described by Gross and co-workers [32,33]. While there is some preference for fragmentation at proline, glutamic acid and aspartic acid residues, both LID and (high energy) CID spectra in our experience have resulted in nearly complete b- and y-series ions for unmodified peptides. For the lysine acetylated peptides described earlier, MS/MS spectra have also included abundant c-series ions [12], but these are relatively well-distributed across the peptide sequence.

The similarity in spectra obtained by LID and CID in this instrument is also interesting. In instruments that utilize a quadrupole, ion trap or FTMS, in which the ion residence time is relatively long, it is, generally, desirable to inject ions with relatively low internal energy (to prevent immediate dissociation) and low kinetic energy (to enable capture); and these ions are subsequently cooled so that fragmentation does not occur prior to mass selection or isolation. Thus, an important difference in the time-of-flight mass spectrometer is that fragmentation occurring in space and time prior to mass selection does not affect their velocities or the ability to isolate/select associated precursors and products. In that case, the imparting of significant internal energy by the MALDI process itself may be important to the success of the CID process, with collisions in effect providing the last needed energy to an already highly excited ion. The relationship between these processes underscores again the need for recording all of the fragment ions from a mass-selected precursor, whether these dissociate before, during or after the collision.

References

[1] R.J. Cotter, T.J. Cornish, Anal. Chem. 65 (1993) 1043.
[2] T.J. Cornish, R.J. Cotter, Org. Mass Spectrom. 28 (1993) 1129.
[3] B.A. Mamyrin, Int. J. Mass Spectrom. Ion Processes 131 (1994) 1.
[4] R.J. Cotter, Time-of-Flight Mass Spectrometry: Instrumentation and Applications in Biological Research, American Chemical Society, Washington, DC, 1997.
[5] M.A. Seeterlin, P.R. Vlasak, D.J. Beussman, R.D. McLane, C.G. Enke, J. Am. Chem. Soc. 4 (1993) 751.
[6] T.J. Cornish, R.J. Cotter, Rapid Commun. Mass Spectrom. 7 (1993) 1037.
[7] M.M. Cordero, T.J. Cornish, R.J. Cotter, J. Am. Soc. Mass Spectrom. 7 (1996) 590.
[8] R. Kaufmann, D. Kirsch, B. Spengler, Int. J. Mass Spectrom. Ion Processes 131 (1994) 355.
[9] T.J. Cornish, R.J. Cotter, Rapid Commun. Mass Spectrom. 8 (1994) 781.
[10] M.M. Cordero, T.J. Cornish, R.J. Cotter, I.A. Lys, Rapid Commun. Mass Spectrom. 9 (1995) 1356.
[11] P. Thompson, D. Wang, L. Wang, M. Fulco, N. Pediconi, D. Zhang, W. An, Q. Ge, R.G. Roeder, J. Wong, M. Levrero, V. Sartorelli, R.J. Cotter, P.A. Cole, Nat. Struct. Mol. Biol. 11 (2004) 308.
[12] D. Wang, P. Thompson, P.A. Cole, R.J. Cotter, Structural analysis of a highly acetylated protein using a curved-field reflectron mass spectrometer, Proteomics (in press).
[13] R.M. Whittal, L. Li, Anal. Chem. 67 (1995) 1950.
[14] R.S. Brown, J.J. Lennon, Anal. Chem. 67 (1995) 1998.
[15] M.L. Vestal, P. Juhasz, S.A. Martin, Rapid Commun. Mass Spectrom. 9 (1995) 1044.
[16] K. Medzihradszky, J.M. Campbell, M.A. Baldwin, A.M. Falick, P. Juhasz, M.L. Vestal, A.L. Burlingame, Anal. Chem. 72 (2000) 552.
[17] V. Schnaible, S. Wefing, A. Resemann, D. Suckau, A. Bücker, S. Wolfe-Kümmeth, D. Hoffmann, Anal. Chem. 74 (2002) 4980.
[18] R.J. Cotter, B. Gardner, S. Iltchenko, R.D. English, Anal. Chem. 76 (2004) 1976.
[19] K. Gevaert, H. Demol, L. Martens, B. Hoorelbeke, M. Puype, M. Goethals, J. Van Damme, S. De Boeck, J. Vandekerckhove, Electrophoresis 22 (2001) 1645.
[20] L.N. Marekov, P.M. Steinert, J. Mass Spectrom. 38 (2003) 373.
[21] D. Wang, S.R. Kalb, R.J. Cotter, Rapid Commun. Mass Spectrom. 18 (2004) 96.
[22] W.C. Wiley, I.H. McLaren, Science 124 (1956) 817.
[23] M. Karas, F. Hillenkamp, Anal. Chem. 60 (1988) 2299.

[24] K. Tanaka, H. Waki, Y. Ido, S. Akita, Y. Yoshida, T. Yoshida, Rapid Commun. Mass Spectrom. 2 (1988) 151.
[25] J.B. Fenn, M. Mann, C.K. Meng, S.F. Wong, C.M. Whitehouse, Science 246 (1989) 64.
[26] F. Hillenkamp, E. Unsold, R. Kaufmann, R. Nitsche, Nature 256 (1973) 119.
[27] L. Li, D.M. Lubman, Anal. Chem. 60 (1988) 1409.
[28] J.-C. Tabet, R.J. Cotter, Anal. Chem. 56 (1984) 1662.
[29] R.D. Macfarlane, D.F. Torgerson, Science 191 (1976) 920.
[30] P. Håkansson, M.J. Chalmers, J.P. Quinn, M.A. McFarland, C.L. Hendrickson, A.G. Marshall, Anal. Chem. 75 (2003) 3256.
[31] S.D.-H. Shi, M.E. Hemling, S.A. Carr, D.M. Horn, I. Lindh, F.W. McLafferty, Anal. Chem. 73 (2001) 19.
[32] M.L. Gross, Int. J. Mass Spectrom. 200 (2000) 611.
[33] M. Rosario, M. Domingues, G.O.S. Marques, C.A.M. Vale, M.G. Neves, J.A.S. Cavaleiro, A.J. Ferrer-Correia, O.V. Nemirovskiy, M.L. Gross, J. Am. Soc. Mass Spectrom. 10 (1999) 217.